

Supplementary Information

Direct Current Generation in Triboelectric Nanogenerators Through Ionic Dynamics and Electrode Polarization Effects

Gerald S. Gbadam¹, Hyosik Park¹, Cheoljae Lee¹, Hyeonseo Joo¹, Sujeong Gwak¹, Hong-Joon Yoon², Hanjun Ryu³ and Ju-Hyuck Lee^{1,4}*

¹Department of Energy Science and Engineering, Daegu Gyeongbuk Institute of Science and Technology (DGIST), Daegu 42988, Republic of Korea.

²Department of Electronic Engineering, Gachon University, Seongnam-si, Gyeonggi-do 13120, Republic of Korea

³Department of Advanced Materials Engineering, Chung-Ang University, Anseong, 17546, Republic of Korea; Department of Intelligence Energy and Industry, Chung-Ang University, Seoul, 06974, Republic of Korea

⁴Energy Science and Engineering Research Center, Daegu Gyeongbuk Institute of Science and Technology (DGIST), Daegu 42988, Republic of Korea

Corresponding Author

*E-mail address: jhlee85@dgist.ac.kr

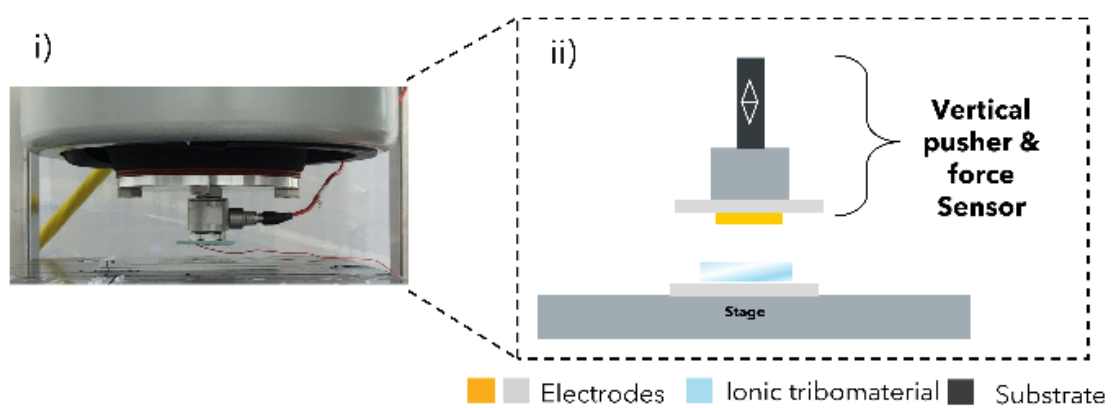


Figure 1. (i) Photograph and (ii) Schematic of the mechanical pusher and force sensor system

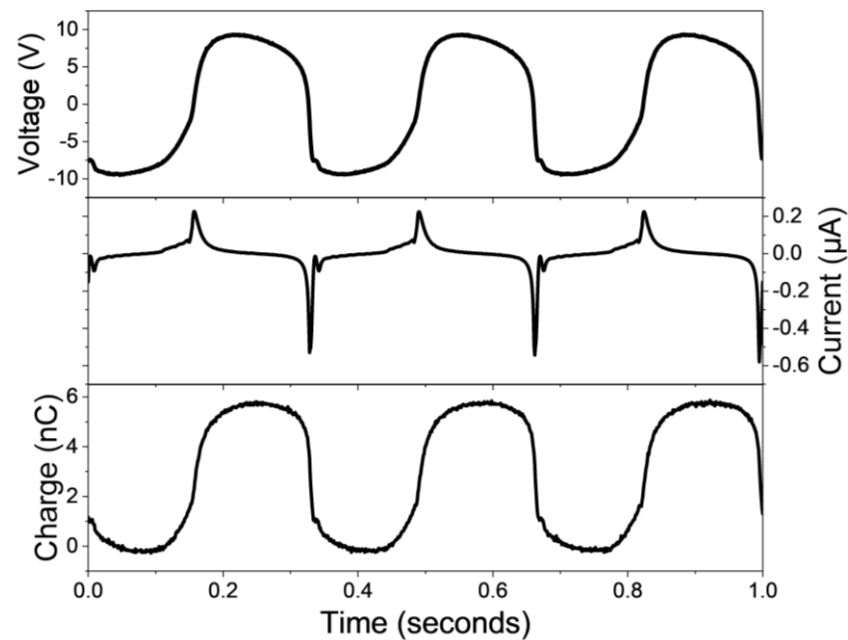


Figure 2. Output of conventional TENG using PVC in conductor-dielectric structure

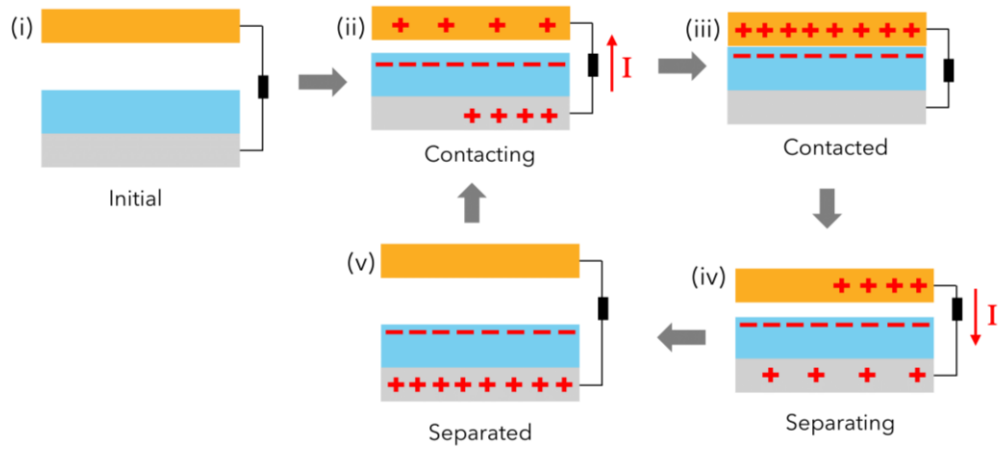


Figure 3. Conventional TENG mechanism using PVC

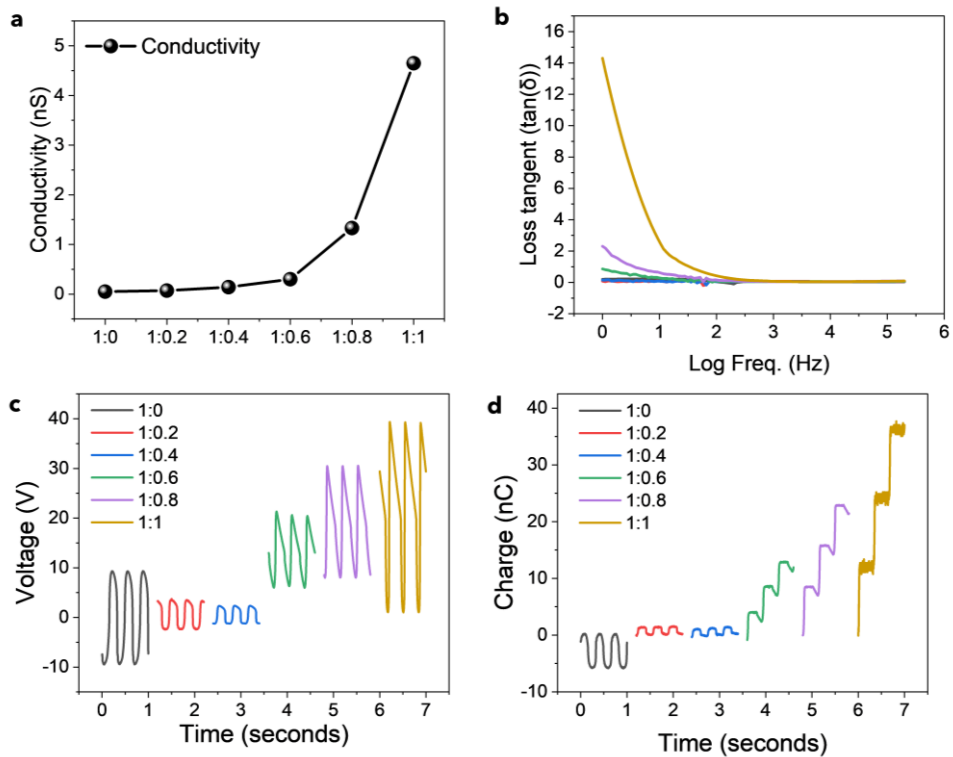


Figure 4. (a) Conductivity, (b) loss tangent (c) Voltage, and (d) Transferred charge of transition from AC to DC (PVC to DOA1)

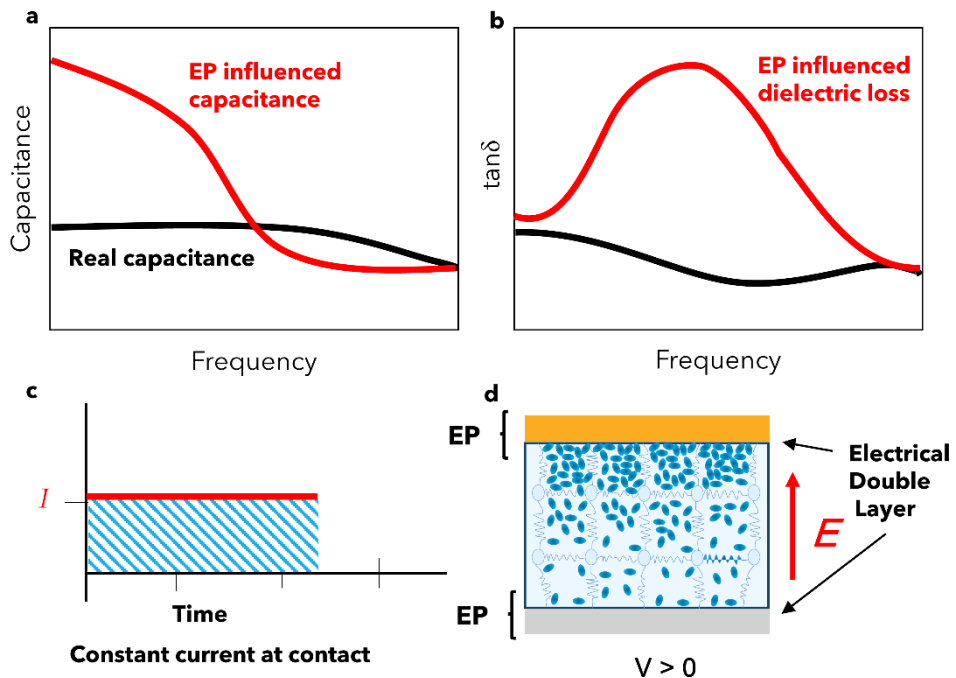


Figure 5. Description of Electrode Polarization a) capacitance b) Dielectric loss curves c) distribution of ions in the films d) Distribution of ions in film cross section showing formation of EDL and electrode interface

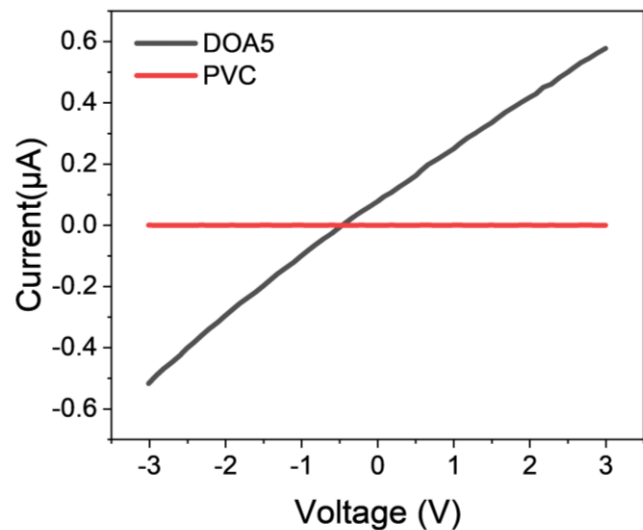


Figure 6. IV Curve of PVC & plasticized PVC (DOA5)

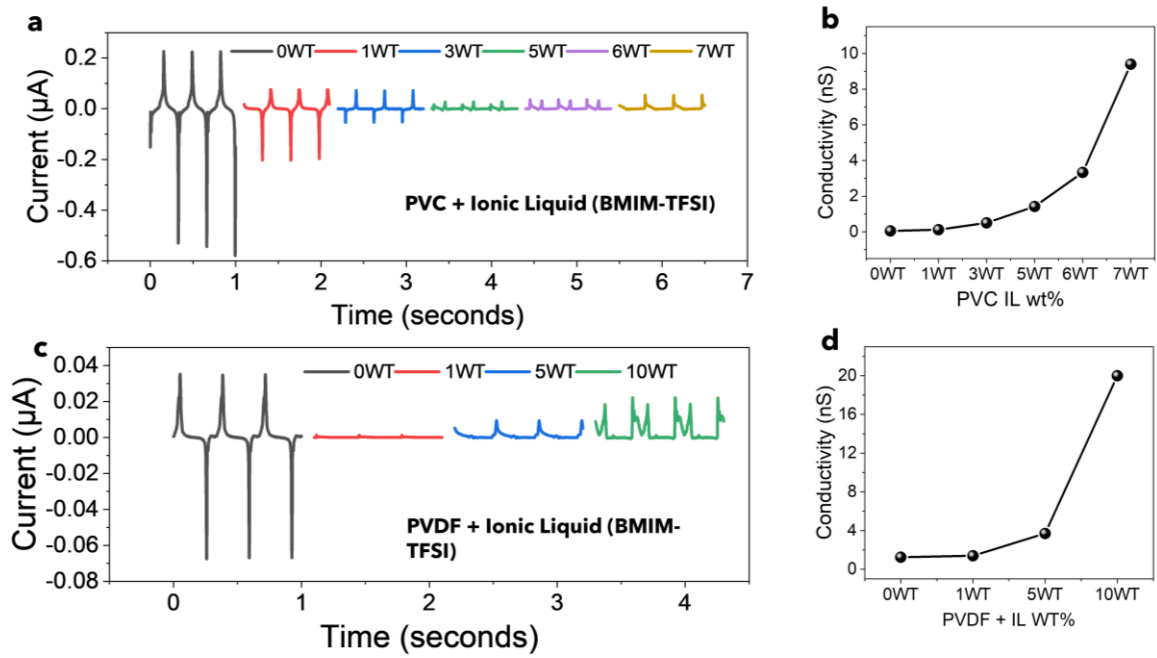


Figure 7. Transient AC-DC behavior as conductivity increases in different materials (a)(b)

PVC +IL (c)(d) PDMS +IL

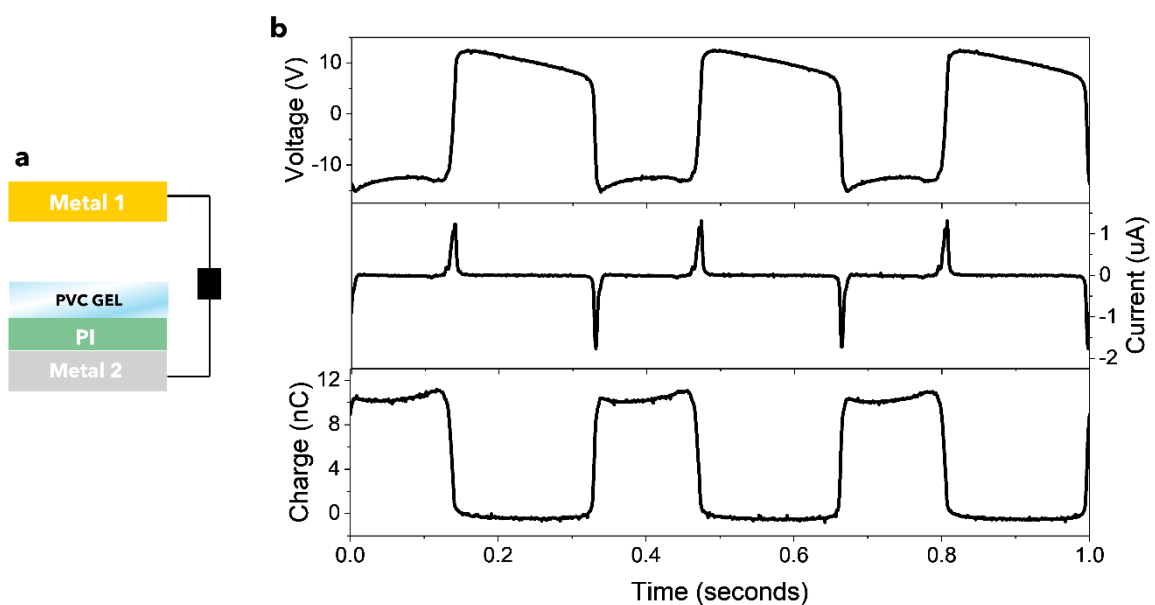


Figure 8. Using a blocking layer with PVC Gel showing AC output owing to the Insulation between the two friction layers

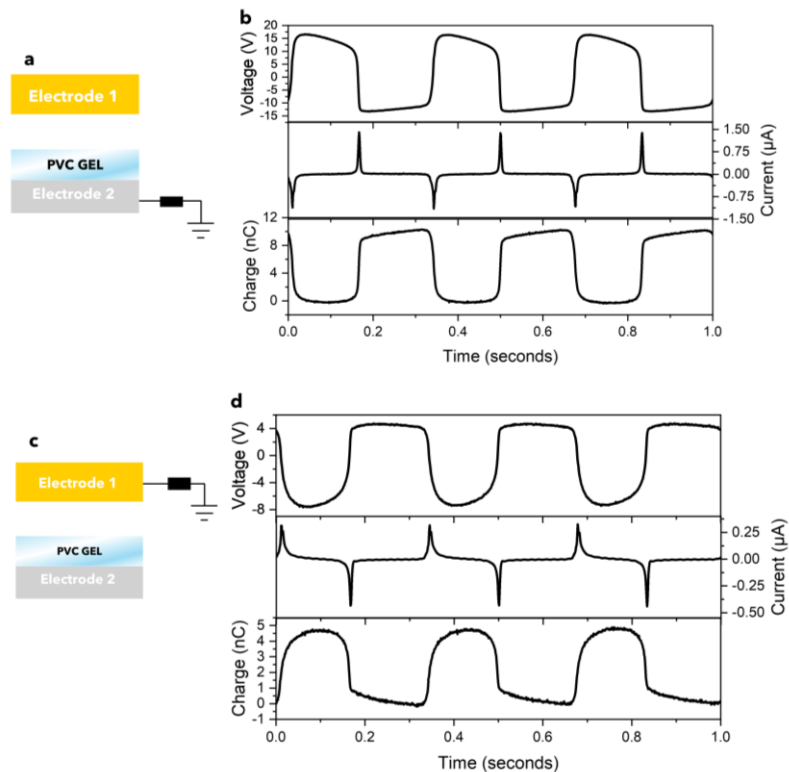


Figure 9. Open-circuit voltage and short-circuit current and transferred charge for plasticized PVC in metal-dielectric-metal mode- single electrode mode

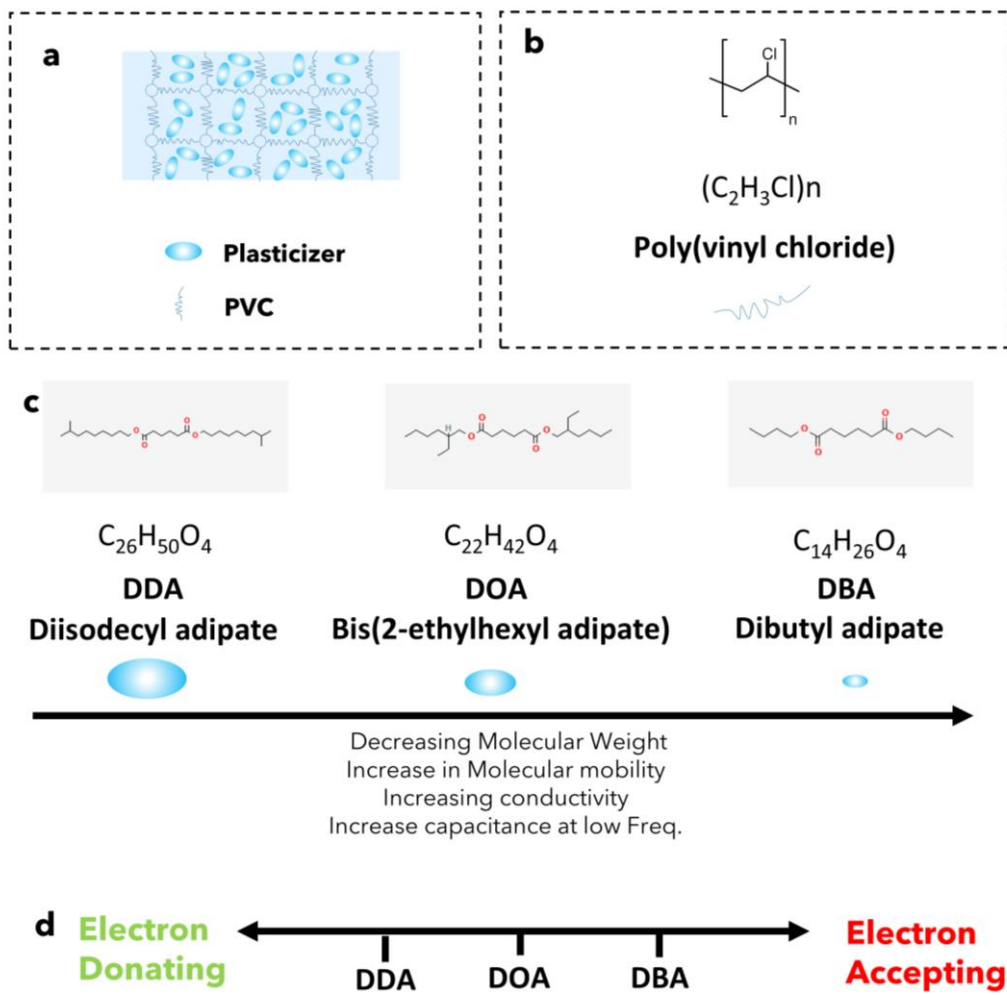


Figure 10. PVC and plasticizer chemical structure and properties (a) PVC and plasticizer Gel structure (b) PVC chemical structure (c) Adipate plasticizer chemical structure correlated with properties and tendencies (d) Triboelectric series depending on plasticizer

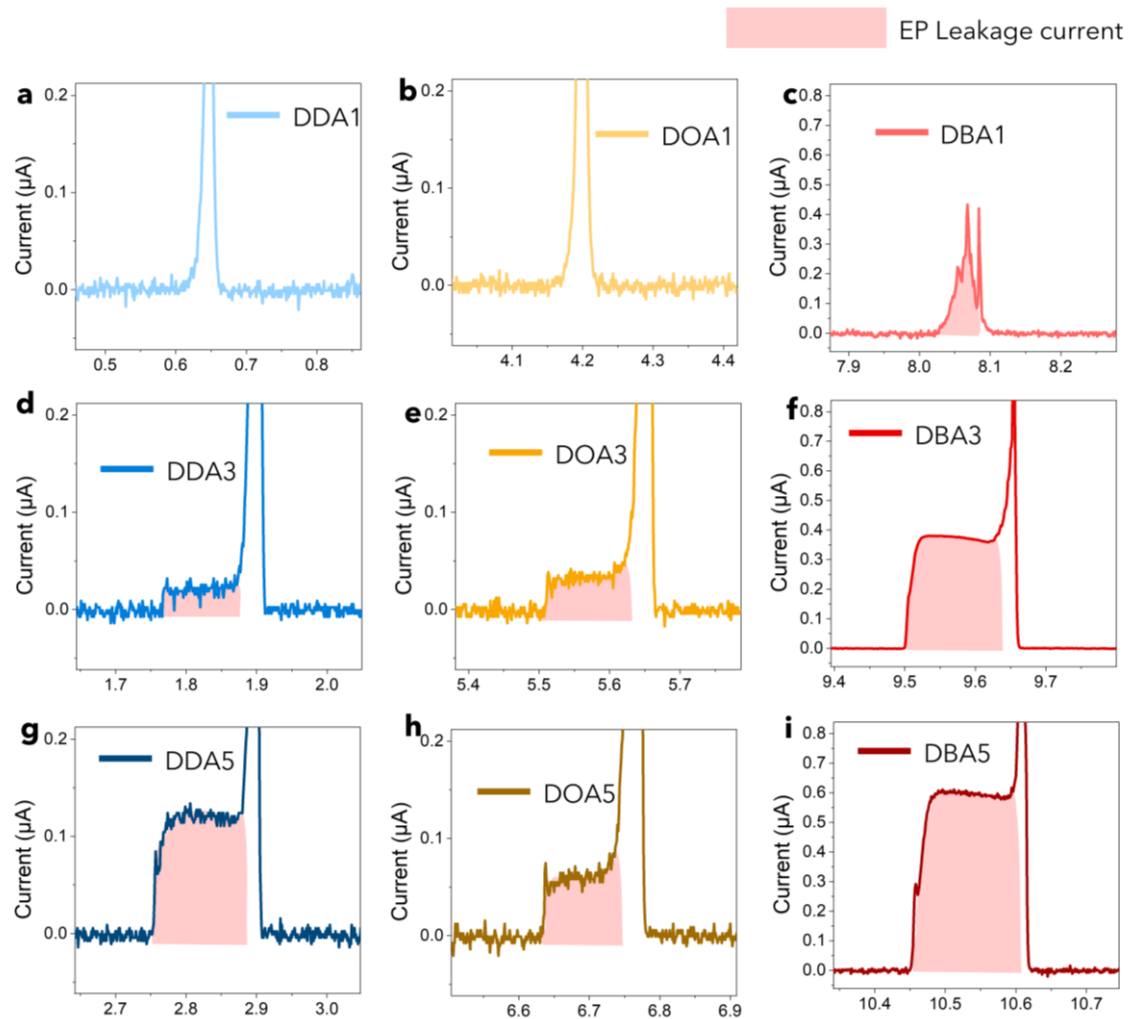


Figure 11. Magnification of contact period during contacting stage in the iDC-TENG comparing various plasticizer and ratios

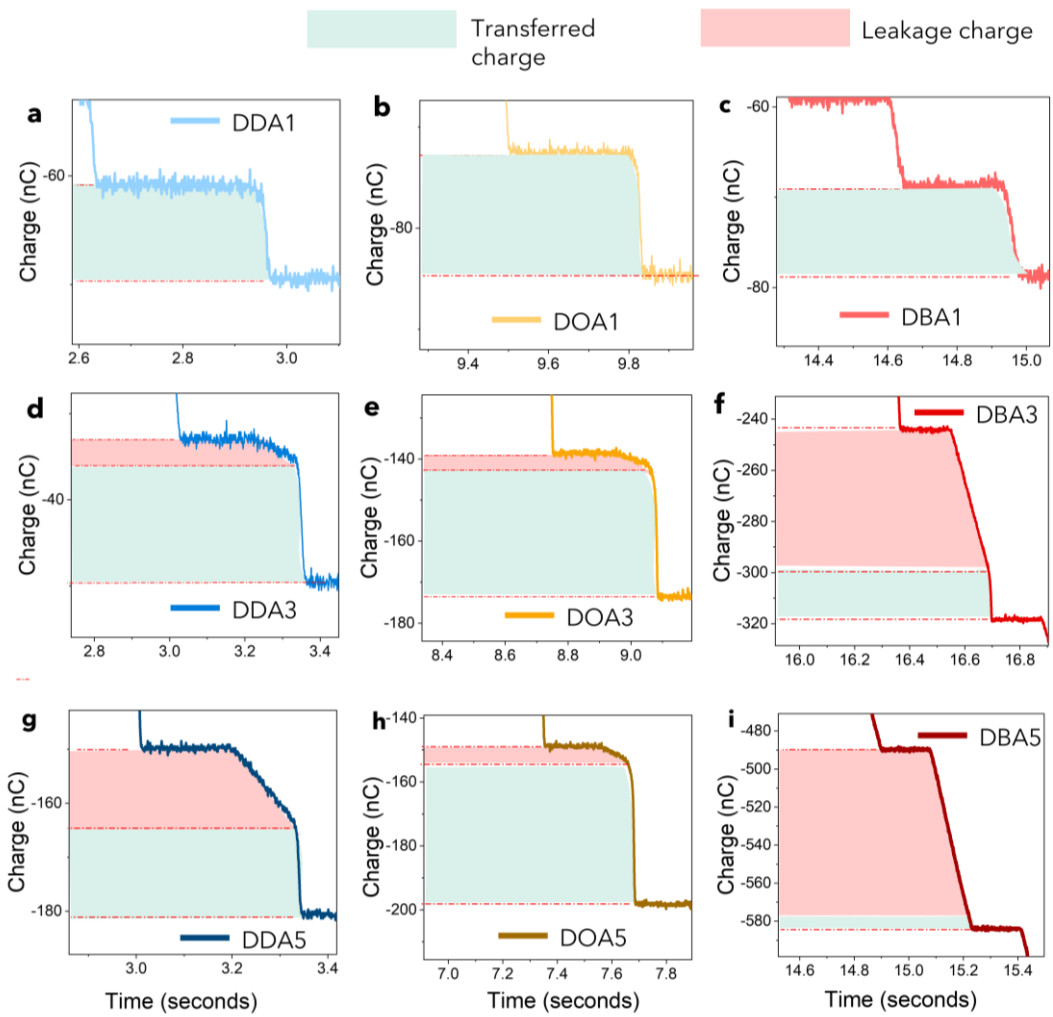


Figure 12. Comparing charge transferred and charge leakage from the various films

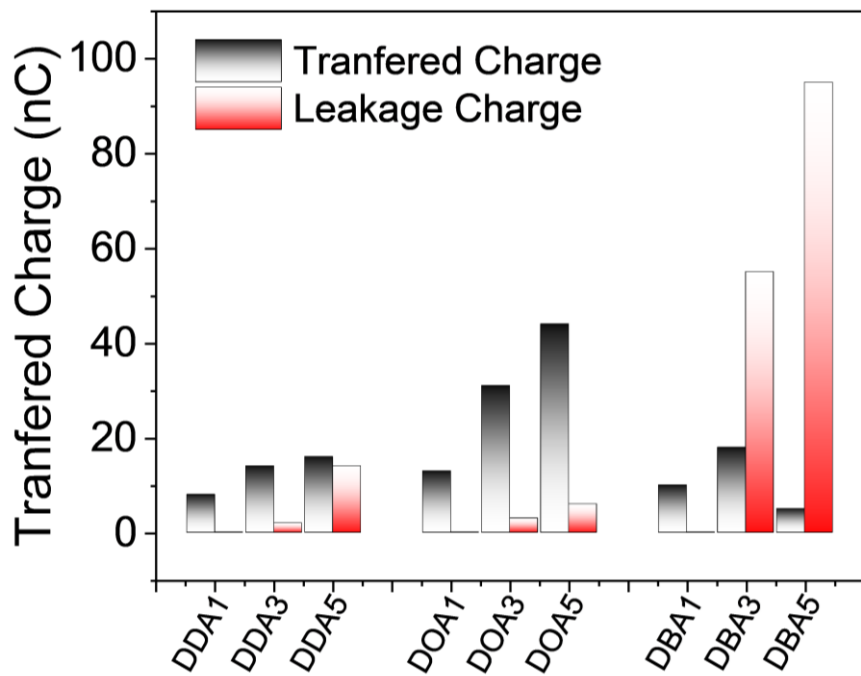


Figure 13. Transferred charge and leakage output form in once cycle for all films

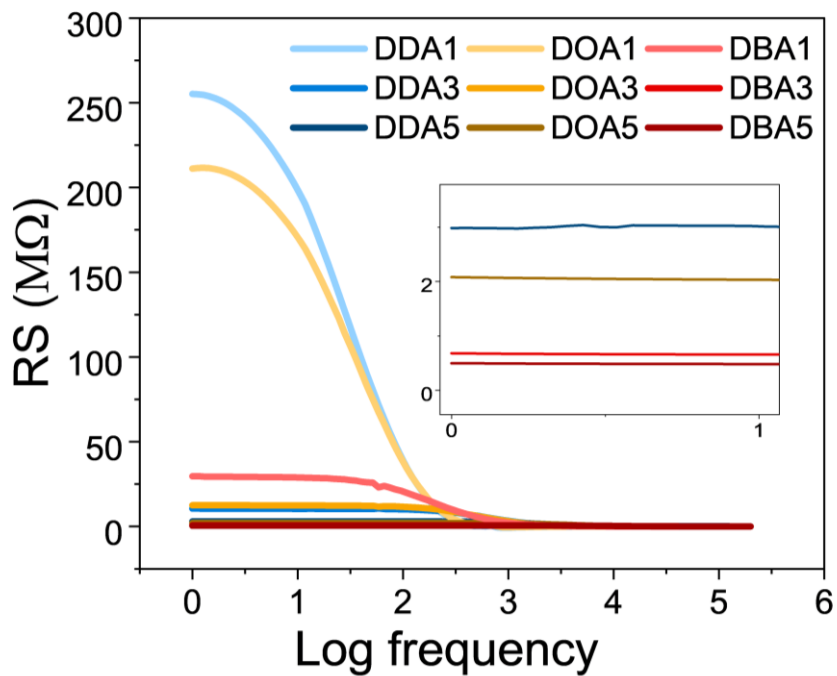


Figure 14. Resistance plot of various films over frequencies from 0 hz to 200 khz

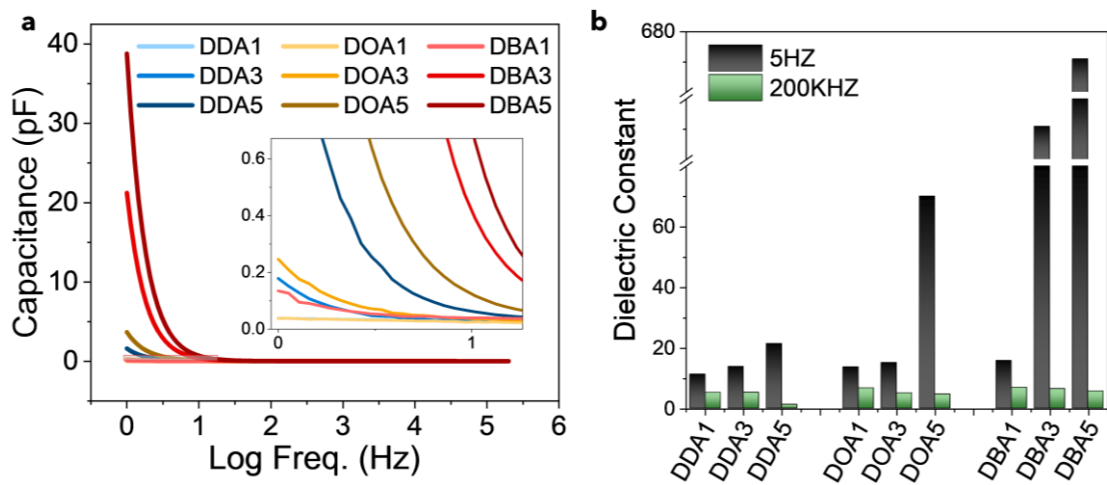


Figure 15. a) Capacitance and b) Dielectric constant plot of various films over frequencies from 0 hz to 200 khz

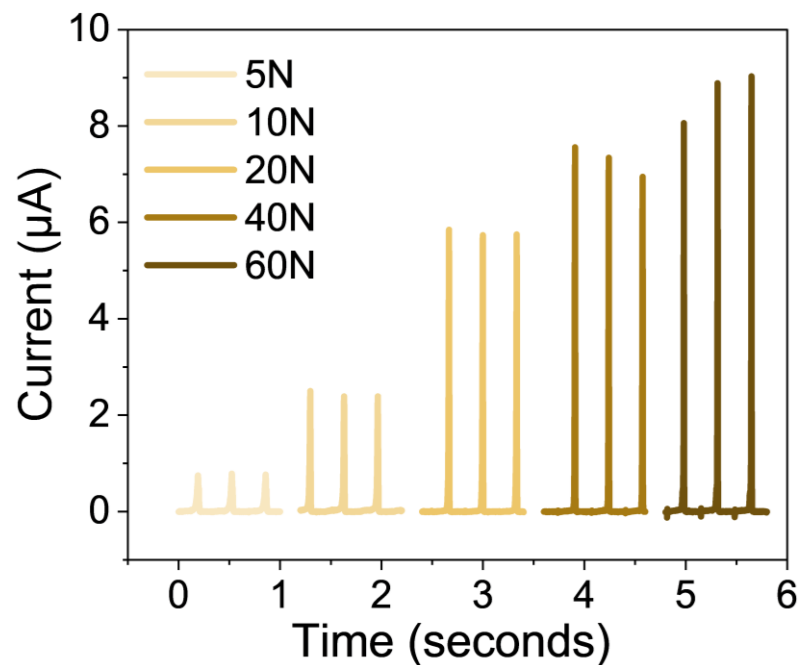


Figure 16. Current output for force from 5 N to 60 N

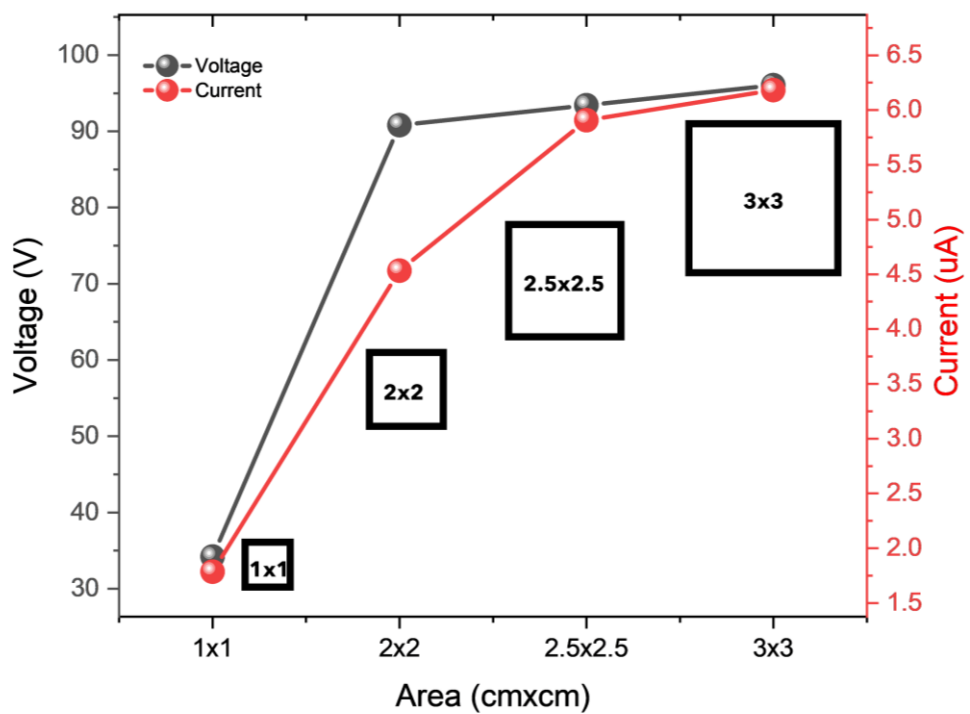


Figure 17. Area Dependence of contact-separation iDC-TENG

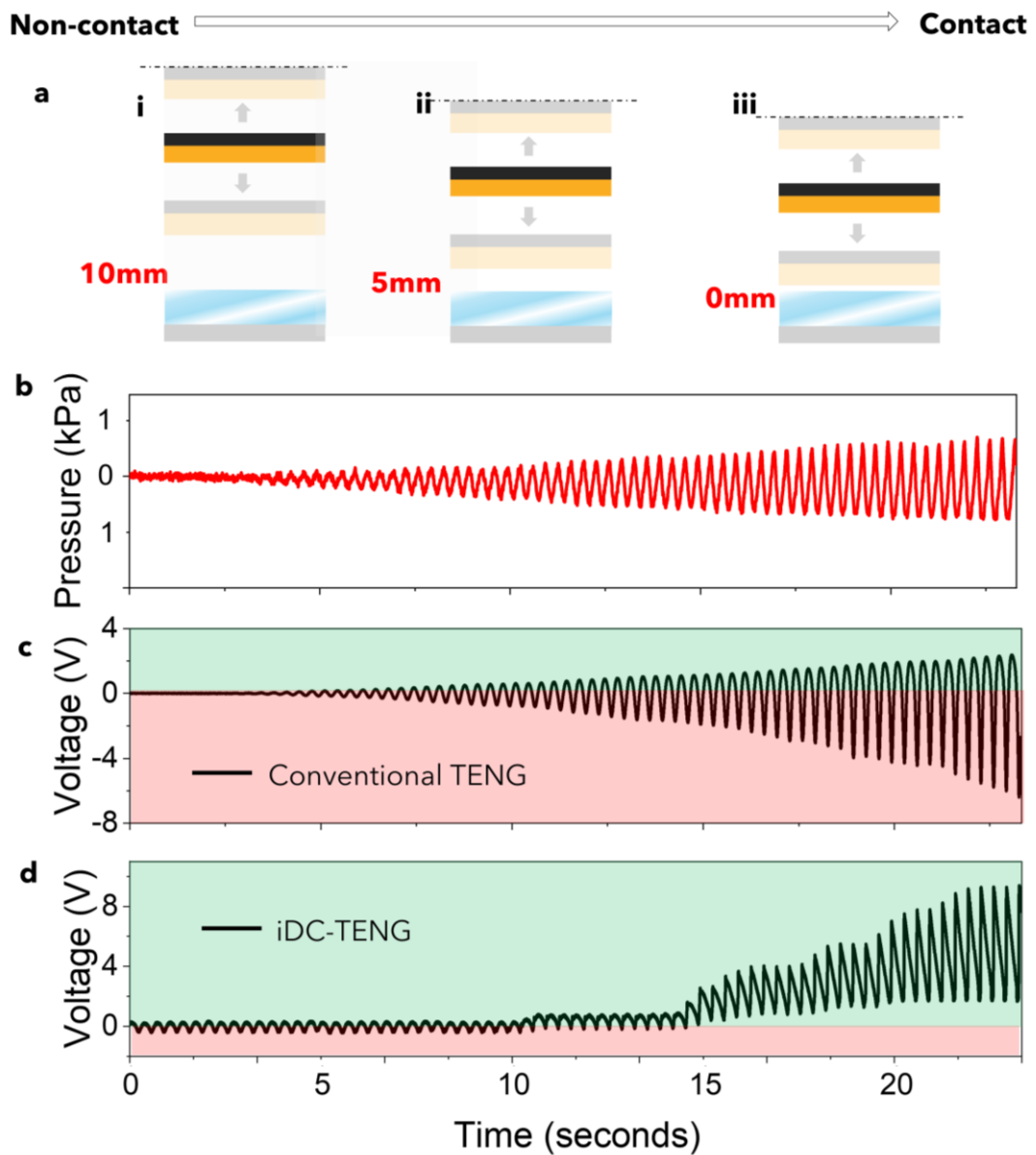


Figure 18. Non-contact to contact voltage sweep (a) Schematic of non-contact to contact sweep from 10mm oscillation gap to 0mm gap (a) pressure sensor values open-circuit voltage of (c) PVC and (d) plasticized PVC as triboactive material

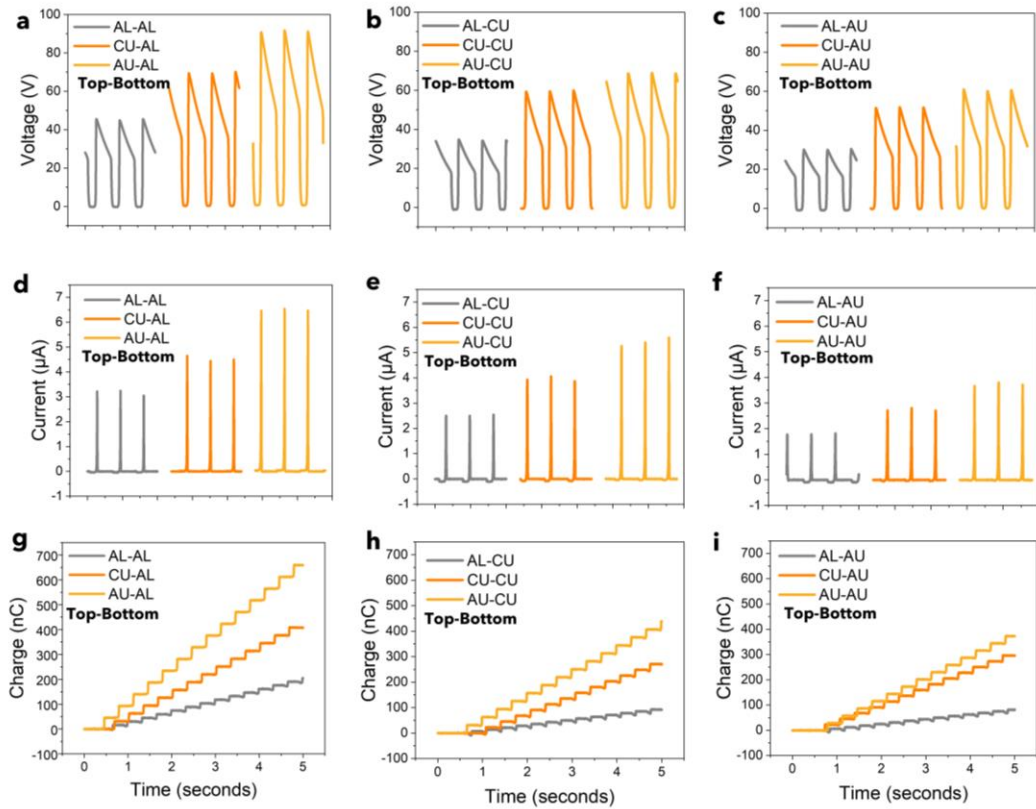


Figure 19. Output voltage and current of electrode work function dependence

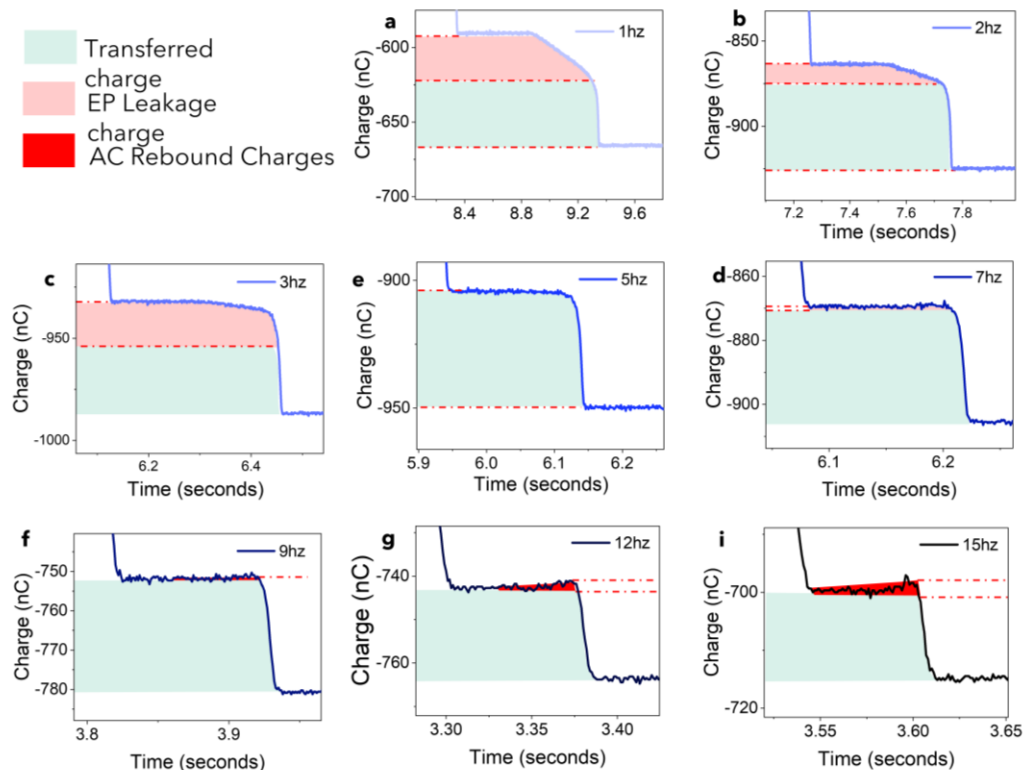


Figure 20. Transferred charge of the frequency dependence

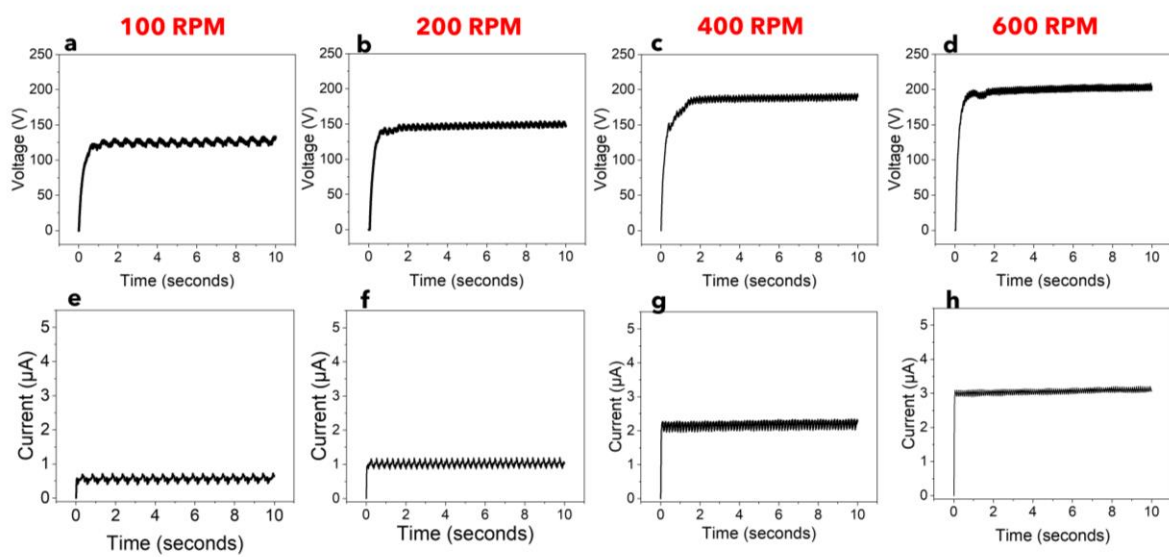


Figure 21. Voltage, current and transferred charge of PVC gel-based rotary DC TENG of 12 segments at different speeds

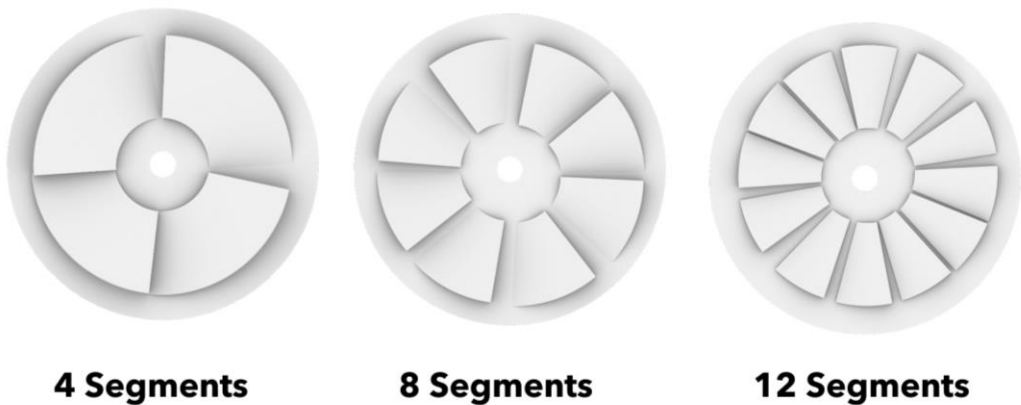
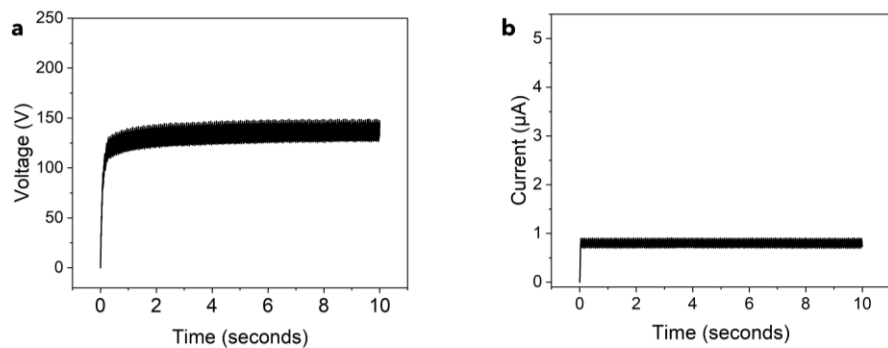


Figure 22. Variant segmentation of flap-based iDC-RTENG

4 Segment



8 Segment

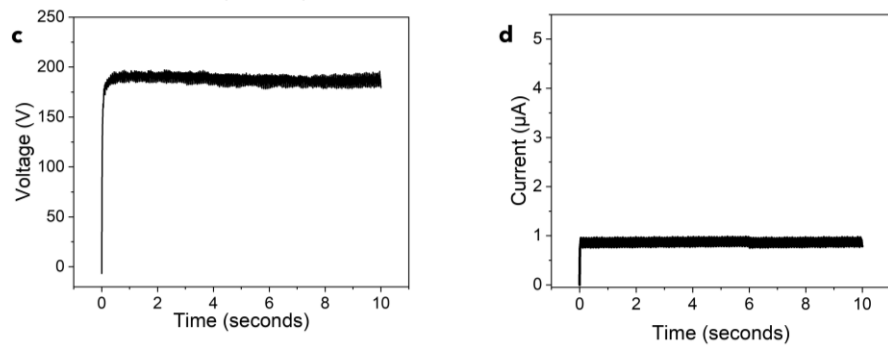


Figure 23. Variant segmentation of flap-based iDC-RTENG

Supplementary Notes:

Note 1 Electrode Polarization

Electrode polarization (EP) is a significant challenge in measuring high-conductivity samples due to the ionic content of conductive ionic films.^{1, 2} EP, marked by charge accumulation at the electrode-ionic film interface, distorts real capacitance (and resistance) measurements, as shown in Figure S5a (Supporting Information). The $\tan\delta$, Dielectric loss (Figure S5b, Supporting Information) shows the extent of attenuation fueled by the dissipation of electrical energy by complex processes. EP has formed the basis for applications like actuation observed in PVC Gel films³. In TENG systems, EP creates a static output influenced by the electric field, as depicted in Figure S5c and Figure S5d (Supporting Information). At lower frequencies, EP obstructs the true behavior of the bulk film, leading to inaccuracies in electrical property measurements.

EP is affected by electrode size, measurement frequency, current density, temperature, electrode roughness, and electrode separation⁴. Methods to mitigate EP include using blocking layers, as demonstrated in Figure S8 (Supporting Information), which disrupt the interface and minimize EP. Although EP has been overlooked in TENGs due to the poor performance of conductive materials, recent developments in iDC-TENGs and tribovoltaic systems necessitate its consideration. Our study shows EP as a baseline phenomenon in producing DC electricity from ionic materials, with its impact influenced by factors like work function orientation and frequency. Plasticized PVC's unique electrical behavior, including EP, parallels what we observe in TENG systems. By controlling EP, we can enhance TENG performance and application. EP is crucial for accurate electrical measurement in high-conductivity samples. Proper management of EP through controlled conditions and innovative methods can improve TENG systems and other applications, underscoring its importance in optimizing electronic performance.

Note 2 Non-contact to contact oscillation sweep

The output peak form is the simplest way by which we can analyze the output of the triboelectric pair behaviour, considering all the various parameters that influence its output. In this study, the output peaks describe the influence of EP on the behaviour of the TENG. We performed a simulation by controlling the distance of the TENG pair (Au and the plasticized PVC) while the pusher was in vertical oscillating motion as shown in Figure S18a (Supporting Information).

There are two primary points of focus in this oscillation sweep during ongoing oscillatory motion: i), ii) when the surfaces do not come into contact, and iii) when the surfaces do come into contact during the vertical oscillating motion. At 0 mm distance is when contact is made during the oscillation, and as we have described, EP can only take place at contact, conversely contact electrification leading to electrostatic induction can produce an output even without contact because the varying electric field increases as the separation distance increases between the dielectric layer and the electrode. Therefore, in the non-contact mode of all materials, with or without EP, we expect to observe the characteristic behavior of contact electrification. This oscillation sweep effectively clarifies the behavior and the transition from AC to DC upon the introduction of electrode polarization at contact. Initially, there is no perceived force or contact (Figure S18b, Supporting Information), and the voltage output peaks show AC behavior in both the conventional TENG (Figure S18c, Supporting Information) and iDC-TENG (Figure S18d, Supporting Information).

In a conventional TENG with the metal-dielectric-metal mode (such as using PVC), shown in Figure S18c (Supporting Information), the sinusoidal AC output is continuous, with only its magnitude changing as the separation distance decreases. However, with introduction of the EP effect at contact, the output is suppressed during the contact stage and changes in magnitude only during the separation stage as can be seen in the output of iDC-TENG.

For iDC-TENG (Figure S18d, Supporting Information), when the oscillation has an extended separation distance of (i) 10mm gradually reduced to contact at (iii) 0 mm, we notice a change in peak generation. Initially, there is no perceived force or contact (Figure S18b, Supporting Information), and the voltage output peaks show AC behavior. Right at the point where contact is made, there is a transition point to the DC output. The electric field sinusoidal waveform is changed due to the EP effect which nullifies the output at the point of contact.

Note 3 Modified TENG equation

For mobile ions in a dielectric film, Poisson's equation⁵ shows that, in steady-state

$$\frac{dE(x)}{dx} = \frac{\rho(x)}{\epsilon}$$

where $E(x)$ is the electric field across the film, $\rho(x)$ is the ion concentration and ϵ is the permittivity. This equation indicates that the presence of ions in the film can influence the electric field. Further,

$$E = E_{bi} \propto V_{bi} \propto \Delta\phi$$

$$\text{and } \Delta\phi = \phi_1 - \phi_2$$

where V_{bi} is the built-in potential across the film emanating from the difference in the work function (ϕ) of the electrodes. Note that the values are stated as scalar quantities for simplicity but are vectors in principle. The V-Q-x relation for TENG in m-d-m is given by⁶

$$V = Ed + E_{air}x$$

The electric field strength in the dielectric d , $E = \frac{-Q}{S\epsilon_0\epsilon_1}$, and inside the air gap $E_{air} = \frac{-Q}{S\epsilon_0} +$

$$\frac{\sigma(t)}{\epsilon_0}$$

$$\text{Therefore, } V = -\frac{Q}{S\epsilon_0} \left(\frac{d}{\epsilon_r} + x(t) \right) + \frac{\sigma x(t)}{\epsilon_0}$$

Due to EP leakage, we can account for the charges on d as $S\sigma - Q$

The Electric field strength is given (for EP Leakage case)

In dielectric 1 (modified)

$$E = \frac{-S\sigma - Q}{S\epsilon_0\epsilon_r}$$

Therefore, the modified V-Q-x relationship for the iDC-TENG (EP Leakage case)

$$V = \left(\frac{-S\sigma - Q}{S\epsilon_0\epsilon_r} \right) d + \left(\frac{-Q}{S\epsilon_0} + \frac{\sigma(t)}{\epsilon_0} \right) x$$

$$V = \frac{-\sigma d}{\epsilon_0 \epsilon_r} + \frac{Q}{S \epsilon_0} \left(\frac{d}{\epsilon_r} - x \right) + \frac{\sigma x(t)}{\epsilon_0}$$

The modified equation now includes the term $\frac{-\sigma d}{\epsilon_0 \epsilon_r}$, which accounts for the EP leakage effect in the dielectric film. The built-in potential V_{bi} , proportional to $\Delta\phi$, impacts the effective charge density (σ). Therefore, we can denote this effect as $\sigma' = \sigma + \beta\Delta\phi$, where β is a proportionality constant.

Final Modified equation

$$V = \frac{-\sigma' d}{\epsilon_0 \epsilon_r} + \frac{Q}{S \epsilon_0} \left(\frac{d}{\epsilon_r} - x \right) + \frac{\sigma' x(t)}{\epsilon_0}$$

$$\text{Expanded form, } V = \frac{-(\sigma + \beta\Delta\phi) d}{\epsilon_0 \epsilon_r} + \frac{Q}{S \epsilon_0} \left(\frac{d}{\epsilon_r} - x \right) + \frac{(\sigma + \beta\Delta\phi) x(t)}{\epsilon_0}$$

Implications for Q_{sc}

$$Q_{sc} = \frac{S(\sigma + \beta\Delta\phi)x(t)}{d_0 + x(t)}$$

At short-circuit conditions, where the voltage V is zero, the transferred charge Q_{sc} reflects the influence of the built-in electric field due to the difference in work functions of the electrodes. At contact, this built-in electric field contributes to Q_{sc} by affecting the charge distribution and the leakage effect in the dielectric layers. This contribution, which is not captured in simpler models, is represented by the additional charge density term $(\sigma + \beta\Delta\phi)$. As the electrodes separate, the built-in electric field continues to affect the transferred charge Q_{sc} , highlighting its role in both initial charge transfer and subsequent separation. This demonstrates how the built-in electric field significantly impacts the TENG's performance, with the leakage and work function differences influencing the output charge.

Note 4 Crest Factor equation

To describe and compare the uniformity of DC output from electrical systems, the crest factor is the mathematical parameter used to describe the waveform. A perfect crest factor represents a constant voltage or current with no outlier peaks from the maximum peak. The crest factor (CF) equation for the current output is given by:

$$CF = \frac{I_{peak}}{I_{RMS}}$$

$$\text{where } I_{RMS} = \sqrt{\frac{1}{n} \sum_{i=1}^n I_i^2}$$

In our study, we investigated the output of the iDC-RTENG by examining the waveform as the number of segments changed. As the number of segments increased, not only did the magnitude of the output increase, but the CF also improved, achieving a CF of 1.02 with the 12 segmented iDC-RTENG, as shown in Figure 6h. The increased number of segments led to a cumulative effect due to more collisions and sliding of the friction surface, resulting in improved uniformity. It is expected that variance in speed would also alter the CF. With increased speed, the CF is reduced, adhering to the same principle and mechanism.

Supplementary References

1. Iannarelli A, Niasar MG, Ross R. Electrode interface polarization formation in dielectric elastomer actuators. *Sensor Actuat a-Phys* **312**, (2020).

2. Ishai PB, Talary MS, Caduff A, Levy E, Feldman Y. Electrode polarization in dielectric measurements: a review. *Measurement Science and Technology* **24**, (2013).
3. Ali M, Hirai T. Relationship between electrode polarization and electrical actuation of dielectric PVC gel actuators. *Soft Matter* **8**, 3694-3699 (2012).
4. Lata A, Mandal N. Electrode polarization impedance and its application in flow rate measurement of conductive liquid: A review. *IEEE Sensors Journal* **21**, 4018-4029 (2020).
5. Iwamoto M, Mashita K, Hino T. A method for calculating ionic space-charge distribution and its polarization in dielectrics. *Electrical Engineering in Japan* **100**, 8-13 (2007).
6. Niu SM, *et al.* Theoretical study of contact-mode triboelectric nanogenerators as an effective power source. *Energ Environ Sci* **6**, 3576-3583 (2013).